ELSEVIER

Chemical Engineering Science 63 (2008) 4902–4909

Chemical Engineering Science

www.elsevier.com/locate/ces

Sensitivity enhancement and dynamic behavior analysis by modulation excitation spectroscopy: Principle and application in heterogeneous catalysis

Atsushi Urakawa[a,*], Thomas Bürgi[b], Alfons Baiker[a]

[a]*Institute for Chemical and Bioengineering, Department of Chemistry and Applied Biosciences, ETH Zurich Hönggerberg, HCI, 8093 Zurich, Switzerland*
[b]*Université de Neuchâtel, Institut de Microtechnique, Rue Emile-Argand 11, 2009 Neuchâtel, Switzerland*

Received 20 April 2007; received in revised form 31 May 2007
Available online 16 June 2007

Abstract

Modulation excitation spectroscopy (MES) allows sensitive and selective detection and monitoring of the dynamic behavior of species directly involved in a reaction. The method, combined with proper *in situ* spectroscopy, is powerful for elucidating complex systems and noisy data as often encountered in heterogeneous catalytic reactions at solid–liquid and solid–gas interfaces under working conditions. The theoretical principle and actual data processing of MES are explained in detail. Periodic perturbation of the system by an external parameter, such as concentration and temperature, is utilized as stimulation in MES. The influence of stimulation shape upon response analysis is explained. Furthermore, an illustrative example of MES, enantioselective hydrogenation at a solid-liquid interface, is presented.

Keywords: Catalysis; Chemical analysis; Kinetics; Transient response

1. Introduction

Heterogeneous catalysis is the result of various superimposed phenomena. Understanding of catalytic activity and determination of the catalytic active sites in this complex system under working conditions have been and will be a big challenge for those who develop more efficient catalysts by rational design. Recent progress of *in situ* spectroscopy has opened up a wide range of possibilities to monitor various states of species and materials present under reaction conditions (Hunger and Weitkamp, 2001; Weckhuysen, 2002). Despite the recent technical advances, in reality, the interpretation of *in situ* spectroscopic measurements is often a formidable task due to the complexity of catalytic systems. None of the available techniques can, by itself, selectively measure the species responsible for the reaction, i.e. the *active species*, and differentiate them from *spectators* which are not involved in the reaction directly. The presence of spectators, including catalyst support and solvent, is important and has often a dramatic influence on the state of the active sites during reaction. However, the signals originating from spectators are frequently stronger than that of active species, overwhelming the key information of the catalysis.

Transient response techniques are widely applied in the analysis of reaction intermediates and active species or of reaction kinetics by perturbing a catalytic system with external parameter(s). The type of this stimulation is chosen to influence the concentration or kinetics of species of interests. For example, in a temporal analysis of product (TAP) study the concentration and type of inlet gases are carefully selected to achieve the most informative response of the reaction kinetics (Gleaves et al., 1988; Yablonsky et al., 2003). Other examples are step-relaxation (Desamero et al., 2003; Pospíšil et al., 2003) and modulated periodic cycle experiments (Fringeli et al., 2000; Onyestyák et al., 2000; Chenevarin and Thibault-Starzyk, 2004) with stimulations such as concentration and temperature. Ultrafast spectroscopy is also gaining popularity to investigate reaction pathways by directly monitoring transformations after a short pulse stimulation at a reaction timescale (Bauer et al., 2001; Backus et al., 2005). Those transient methods are combined with various spectroscopic techniques to monitor the state of the species of interest and a stimulation is chosen to maximize the changes of the state. Proper selection of the

* Corresponding author. Tel.: +41 44 633 4235; fax: +41 44 632 1163.
E-mail address: urakawa@chem.ethz.ch (A. Urakawa).

0009-2509/$ - see front matter © 2007 Elsevier Ltd. All rights reserved.
doi:10.1016/j.ces.2007.06.009

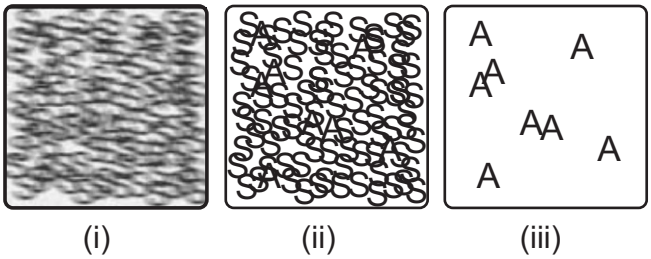

Fig. 1. Three extreme situations of signals obtained by *in situ* spectroscopy of: (i) realistic; (ii) very sensitive; and (iii) very sensitive and selective methods. 'A' and 'S' represent active species and spectators, respectively.

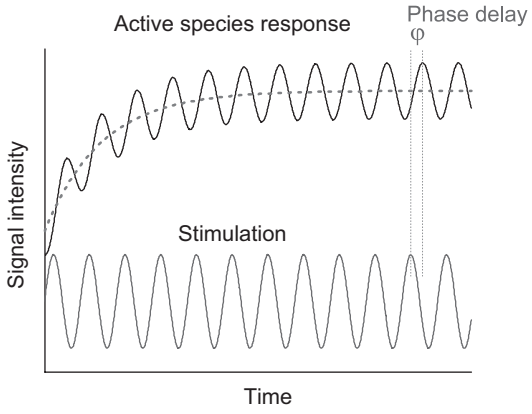

Fig. 2. Typical response of active species affected by a periodic sinusoidal stimulation. Signal intensity and amplitude are arbitrary.

stimulation is crucial; it introduces *selectivity* in observing species of interest. However, the concentration of active species or active sites is typically low and the signal changes introduced by a stimulation are hidden (disguised) by large spectator signals and also noise.

Fig. 1 illustrates a typical situation of *in situ* spectroscopic measurements, where the active and spectator species are denoted as 'A' and 'S', respectively. Such unclear and noisy picture as Fig. 1(i) is obtained by an ordinary method, since one averages their dynamic movements due to the limited sensitivity and also the limited time resolution of the measurements, in addition to unavoidable noise. With an ideally sensitive technique we may improve the limitations and obtain a clear picture, Fig. 1(ii). Yet, the signals of the active species are still overwhelmed by the unwanted spectator signals. A dream *in situ* method would be the one represented in Fig. 1(iii); only the active species can be monitored with high temporal and spatial resolution so that its intrinsic dynamic behavior can be observed.

In this contribution, we explain the machinery of a powerful method, modulation excitation spectroscopy (MES) (Baurecht and Fringeli, 2001), which can greatly reduce the limitations of *in situ* methods towards selective detection of active species as illustrated in Fig. 1(iii), in a time-resolved manner such that the dynamic behavior can also be analyzed accurately. The principle of the method, especially of the mathematical transformation used in the MES, is described in detail, followed by considering the type of stimulation, and finally an illustrative example from heterogeneous catalysis is presented.

2. Principle of MES

MES utilizes a periodic perturbation of a system by external parameter(s), (*stimulation*). A stimulation is chosen to influence the concentration of the target species, which is defined here as, *active species*. Common stimulation parameters are concentration, pH, temperature, light flux, and electric field. Fig. 2 shows a typical response of active species to a sinusoidal stimulation. After some periodic perturbations, the active species concentration reaches a quasi steady-state around which it oscillates, largely at the same frequency as that of the stimulation. The response often shows a phase delay φ with respect to the phase of the stimulation. The amplitude and the phase delay of the response are stimulation-frequency dependent, and contain important information on the *kinetics* of the active species. In general, with increasing frequency the amplitude is decreasing and the phase delay increasing.

One of the main advantages of the periodic operation compared to a step-relaxation experiment is the sensitivity enhancement by averaging the active species signal. The signal after reaching the quasi steady-state can be averaged into one period (e.g. Fig. 3, $A(t)$), thereby improving the signal to noise ratio considerably. By the simple averaging, we can achieve a very high time resolution at which the signal to noise ratio is not sufficient for a single scan.

Further sensitivity enhancement is achieved by a mathematical treatment of the averaged response $A(t)$, a so called *phase-sensitive detection* (*PSD*) or alternatively called *demodulation*, as shown in Eq. (1) (Baurecht and Fringeli, 2001)

$$A_k(\phi_k^{\mathrm{PSD}}) = \frac{2}{T}\int_0^T A(t)\sin(k\omega t + \phi_k^{\mathrm{PSD}})\,\mathrm{d}t, \tag{1}$$

where, T is the length of one period, ω is the stimulation frequency, k is the demodulation index, ϕ_k^{PSD} is the demodulation phase angle for $k\omega$ demodulation, and $A(t)$ and $A_k(\phi_k^{\mathrm{PSD}})$ are the active species response in time- and phase-domain, respectively. Hereafter, in this section we explain in detail the meaning and consequences of the relationship given in Eq. (1). In essence, Eq. (1) converts a time-domain response $A(t)$ to the phase-domain response $A_k(\phi_k^{\mathrm{PSD}})$. The conversion can be carried out at different values of demodulation index k. The choice of k determines which frequency component of the original time-domain response $A(t)$ is obtained by the PSD. For example, when $k = 5$ only the signal oscillating at the frequency of 5ω present in $A(t)$ will show up in the phase-domain response $A_5(\phi_5^{\mathrm{PSD}})$. Mostly, we make only use of the PSD with $k = 1$, since the ω component is dominant or major in a sinusoidal or square-wave stimulation, respectively, resulting in a large ω frequency response. The principle is similar to autocorrelation, Fourier transformation, and the theory of digital lock-in amplification. Fig. 3 illustrates how the PSD actually

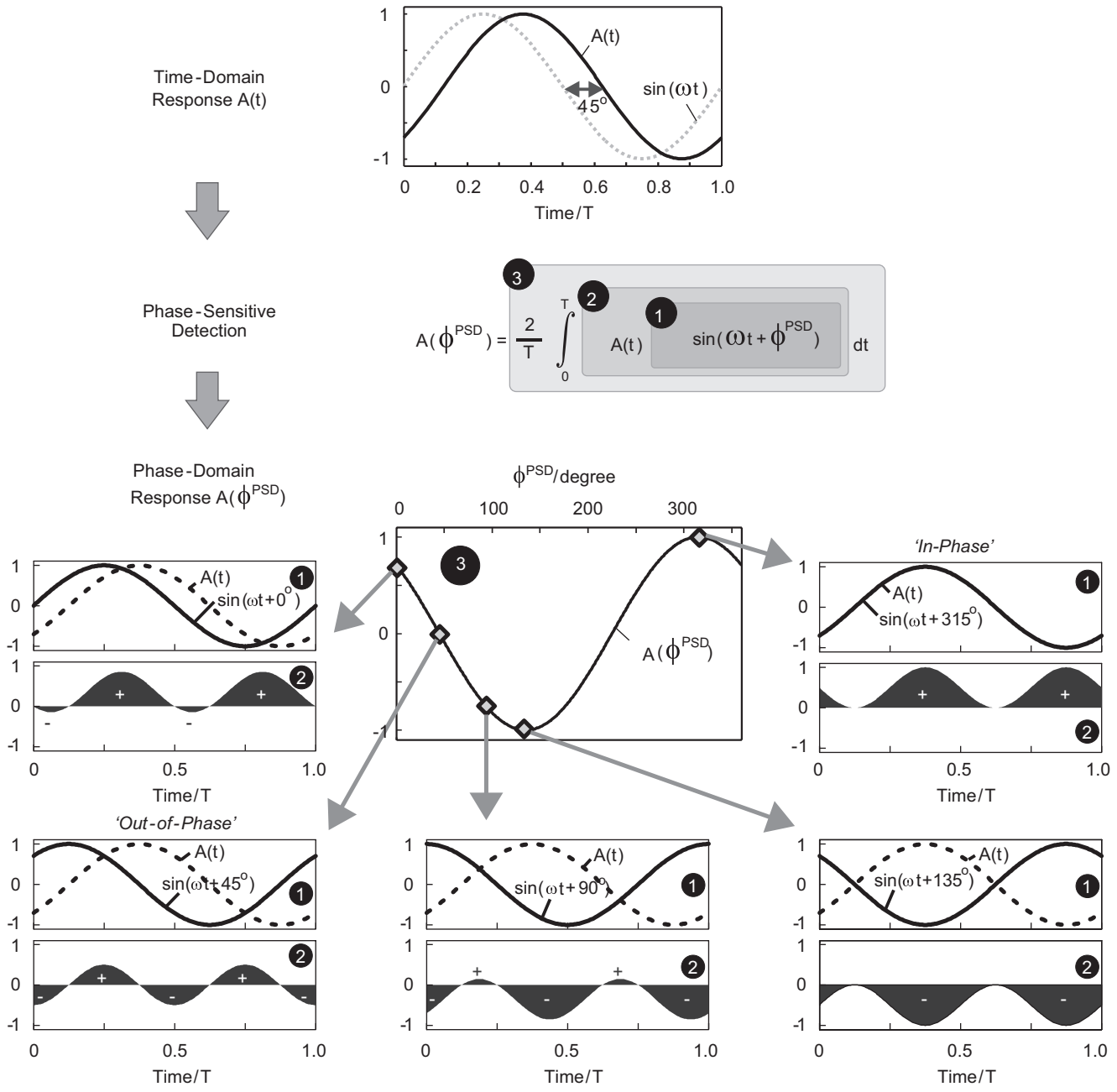

Fig. 3. Phase-sensitive detection (PSD) principle, showing the transformation of time-domain response to the corresponding phase-domain response by PSD. In this model system, the stimulation is $\sin \omega t$ and the time-domain response $A(t)$ is $A \sin(\omega t - 45°)$ with $A = 1$ for simplicity. The phase-domain response show zero amplitudes at 45° and 225° (out-of-phase angle) and become maximum at 315° (in-phase angle).

converts a time-domain response $A(t)$ of active species to the phase-domain response $A(\phi^{\mathrm{PSD}})$. For simplicity, we consider only the major frequency component of the response (it is the exclusive component in this particular case due to the assumed linear response to a sinusoidal stimulation) of fundamental frequency $k\omega$. We suppose that the time-domain response $A(t)$ is a sinusoidal-wave with a phase delay φ of 45°, $\varphi = -45°$, with respect to the stimulation $\sin \omega t$,

$$A(t) = A \sin(\omega t + \varphi), \tag{2}$$

where A is the amplitude of the active species response. The PSD first multiplies $A(t)$ with a sine function of the same frequency with a phase delay of (forward shifted by) ϕ^{PSD} (Fig. 3, ①), which is generally varied from 0° to 360°. When $\phi^{\mathrm{PSD}} = 0°$, the multiplication yields a sine function with 2ω frequency with more positive components (Fig. 3, $\phi^{\mathrm{PSD}} = 0°$, ②), resulting in $A(0°) = 0.71$ after the integration and normalization shown in ③ of the PSD equation. Initial increase in ϕ^{PSD} decreases the value of $A(\phi^{\mathrm{PSD}})$. When $\phi^{\mathrm{PSD}} = 45°$, the phase-domain response $A(\phi^{\mathrm{PSD}})$ becomes zero. It can be easily seen in

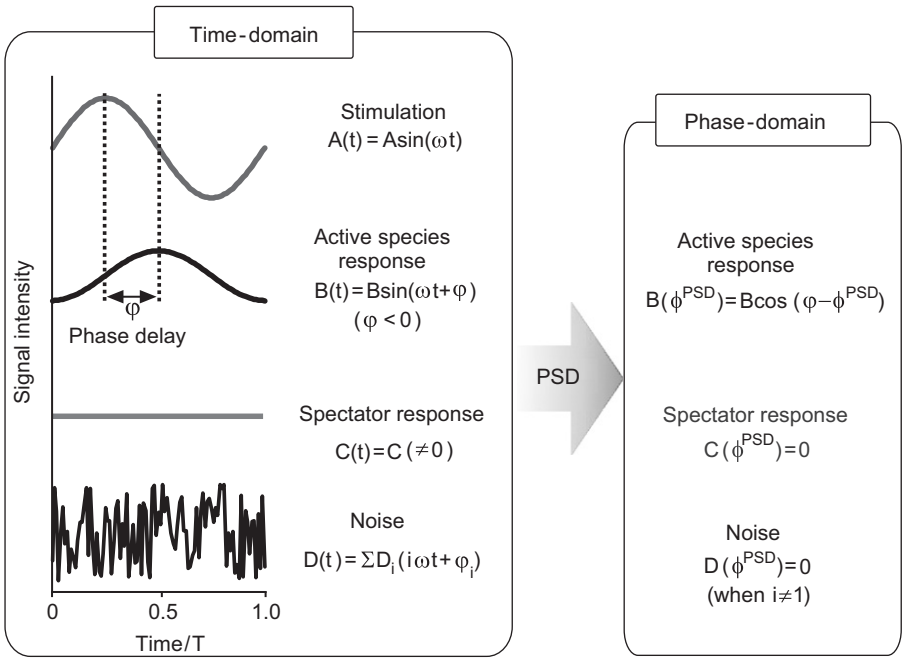

Fig. 4. Schematic illustration of sensitivity enhancement by PSD. $A(t)$: Stimulation function, $B(t)$: response of active species perturbed by the stimulation $A(t)$ where φ is the phase delay with respect to the stimulation, $C(t)$: response of spectator species which is not affected by the perturbation, $D(t)$: Fourier-decomposed noise. The sum of the response components, $B(t) + C(t) + D(t)$, is the actual experimental response.

Fig. 3 that the areas of the positive and negative components of the 2ω frequency-wave after the multiplication ② are equivalent; hence the integration over the period is zero. This demodulation phase angle ϕ^{PSD} yielding zero amplitude is called 'out-of-phase' angle. When we further increase ϕ^{PSD} by 90° from the'out-of-phase' angle, i.e. at $45° + 90° = 135°$, only negative amplitude can be found in the 2ω frequency-wave, resulting in the minimum value, -1, of $A(\phi^{\mathrm{PSD}})$ after the integration ③. The maximum value of $A(\phi^{\mathrm{PSD}})$, 1, is obtained at 180° distant in ϕ^{PSD} from the minimum point of $A(\phi^{\mathrm{PSD}})$, i.e. at $135° + 180° = 315°$, clearly due to the exclusive positive components of the 2ω frequency-wave. The demodulation phase angle ϕ^{PSD} yielding maximum amplitude is called 'in-phase' angle. The phase-domain response can be easily derived analytically (Baurecht and Fringeli, 2001),

$$A(\phi^{\mathrm{PSD}}) = A\cos(\varphi - \phi^{\mathrm{PSD}}). \tag{3}$$

Comparing Eqs. (2) and (3), the main difference between the responses is the domain change; from time- to phase-domain in addition to the function change from sin to cos, retaining the information of the amplitude and phase delay upon the conversion. One may ask what we can benefit from such a transformation if the information of kinetics (A and φ) remains same. In the example of Fig. 3, the signals are indeed equivalent due to the idealized response; however, the advantages become apparent when we deal with more realistic data as described in Fig. 4, with noise and signals from spectator species possibly preventing the detection of a subtle active species response. An actual time-domain response signal can be written as the sum of three components $B(t) + C(t) + D(t)$, where $B(t)$ is the active species response, $C(t)$ is the spectator species response, and $D(t)$ is noise. As mentioned above, information of signals originating from active species remains after the PSD (Eq. (3)). However, spectator species signals, unaffected by the stimulation and remaining constant, are suppressed by the PSD. It is clear from Eq. (1) that when $A(t)$ is constant the phase-domain signal is *zero* after the integration due to the equivalent positive and negative components of the multiplied function. Moreover, the phase-domain signal due to noise, typically possessing higher frequencies than ω, is also *zero*. In other words, the signals due to spectator species and noise present in the time-domain vanish and become invisible in the phase-domain after the PSD, significantly improving the signal to noise ratio of the active species response. As a consequence, in phase-domain the kinetics information, the amplitude and phase delay, can be much more accurately determined than in time-domain.

Also, the sampling efficiency and information obtained by the MES can be greatly enriched by the combination of the PSD with broadband spectroscopy. For example, in FT-IR spectroscopy we obtain a time-domain response as a set of spectra, $A(\tilde{\nu}, t)$, which is then converted to the phase-domain spectra $A(\tilde{\nu}, \phi^{\mathrm{PSD}})$. In the investigation of a reaction A → B → C by modulating the concentration of A, we would observe oscillations of concentration, hence absorbance, of B and C as shown in Fig. 5, showing some phase delay φ of B and C with respect to the stimulation ($\varphi_{\mathrm{B}} = -60$ and $\varphi_{\mathrm{C}} = -150$). The phase-domain spectra at three different phase angles $\phi^{\mathrm{PSD}} = 0$, 210°, and 300° are shown in Fig. 5. The absorbance of A, B, and C become maximum, i.e. 'in-phase', at $\phi^{\mathrm{PSD}} = 0°$, 300°, and 210°, respectively. As discussed in Fig. 3, the bands show zero

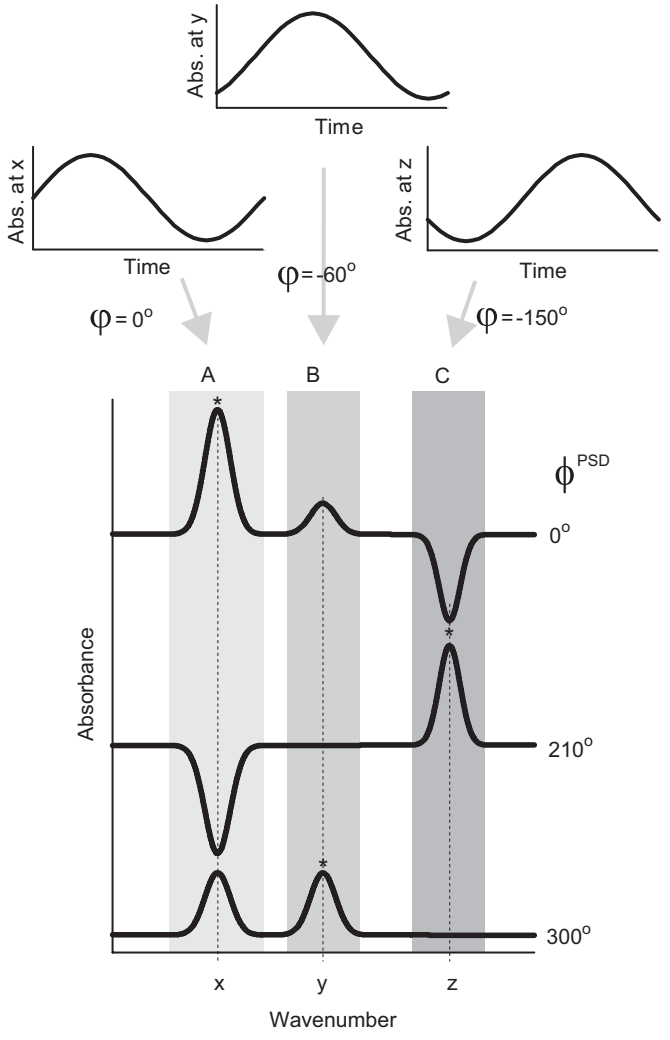

Fig. 5. Kinetic differentiation in IR spectroscopy. The responses are obtained by periodically changing the concentration of A for a consecutive reaction A → B → C. Species A, B, and C have absorbance maxima at x, y, and z, respectively. At this modulation frequency, B and C show 60° and 150° phase delays, respectively. Because of the relation in Eq. (3), the phase domain spectra show maximum amplitudes for B and C at $\phi^{\mathrm{PSD}} = 300°$ and 210°, respectively. The 'in-phase' bands are shown with asterisks.

amplitude at 90° distant from the 'in-phase' angle, as clearly seen from 210° for B and 300° for C. The phase delay and in-phase angle are clearly correlated by Eq. (3), i.e. maximum at $\varphi - \phi^{\mathrm{PSD}} = 0$, hence the phase delay of active species response are readily available from the in-phase angle. The phase-domain spectra using such broadband spectroscopy allow *kinetic differentiation* of stimulation and active species present during the modulation period, that is, species with the same 'in-phase' angle appear at the same time. They may originate from the same species or different species appearing simultaneously. The differentiation of species by means of 'in-phase' angle, hence, phase delay of the species directly gives access to the pathway and lifecycle of active species during a modulation period. In this example (Fig. 5), the reaction pathway A → C via B become evident from the phase-domain spectra. Moreover, screening different modulation frequencies ω will yield information about the kinetics, e.g. rate constants, from the amplitude and phase delay profile of the responses.

3. Shape of stimulation

The illustration of the MES theory above is based on sinusoidal-wave stimulation and corresponding response of the same wave shape (Baurecht and Fringeli, 2001). In practice, square-wave stimulations are largely used in MES since they can be generated often with more ease simply by switching on and off valves for concentration stimulation (Urakawa et al., 2003). It has been validated that the same quantitative and qualitative analysis in phase-domain after the PSD, Eq. (1), can be used using square-wave stimulation (Urakawa et al., 2006a). Moreover, the resulting response contains richer information than using sinusoidal-wave stimulation.

A square-wave with the amplitude of A, $\mathrm{SW}(t)$, can be written as the sum of sinusoidal-waves of odd frequencies.

$$\mathrm{SW}(t) = \frac{4}{\pi}A\left(\sin\omega t + \frac{\sin 3\omega t}{3} + \frac{\sin 5\omega t}{5} + \cdots\right) = \frac{4}{\pi}A\sum_{n=1}^{\infty}\frac{\sin[(2n-1)\omega t]}{2n-1}. \quad (4)$$

The response to a square-wave stimulation is therefore the sum of responses to the stimulation of each $(2n-1)\omega$ frequency components. The beauty of the PSD is that we can separately extract the different $(2n-1)\omega$ frequency components of the response by simply setting $k = 2n-1$ in Eq. (1). The amplitude and phase delay of the obtained response by the $(2n-1)\omega$ frequency demodulation can be related to those obtained when a sinusoidal-wave stimulation of amplitude A is used (Urakawa et al., 2006a),

$$\frac{\pi}{4}(2n-1)A^{SW}_{2n-1} = A^{\sin}|_{1\omega'=(2n-1)\omega} \quad (5)$$

$$\varphi^{SW}_{2n-1} = \varphi^{\sin}|_{1\omega'=(2n-1)\omega} \quad (6)$$

where $A^{\sin}|_{1\omega'=(2n-1)\omega}$ and $\varphi^{\sin}|_{1\omega'=(2n-1)\omega}$ are the amplitude and phase delay of the response to a sinusoidal-wave stimulation at frequency $(2n-1)\omega$, and A^{SW}_{2n-1} and φ^{SW}_{2n-1} are the amplitude and phase delay of the response to a square-wave stimulation at frequency ω but obtained by $(2n-1)\omega$ frequency demodulation. Eqs. (5) and (6) mean that the response obtained by $(2n-1)\omega$ frequency demodulation for square-wave stimulation is equivalent to the response of the sinusoidal-wave stimulation at $(2n-1)\omega$ frequency, except the factor $\pi/4$ and $2n-1$. The former is simply due to the amplitude difference of the fundamental frequency component and the latter is due to the smaller amplitude of higher frequency components in a square-wave. Eqs. (5) and (6) are quantitatively exact only for linear systems, yet it is also valid for non-linear systems when the stimulation amplitude is small enough so that active species respond in a linear manner.

The practical importance of Eqs. (5) and (6) is that one experiment using square-wave stimulation is equivalent to several experiments using sinusoidal-wave stimulation of different

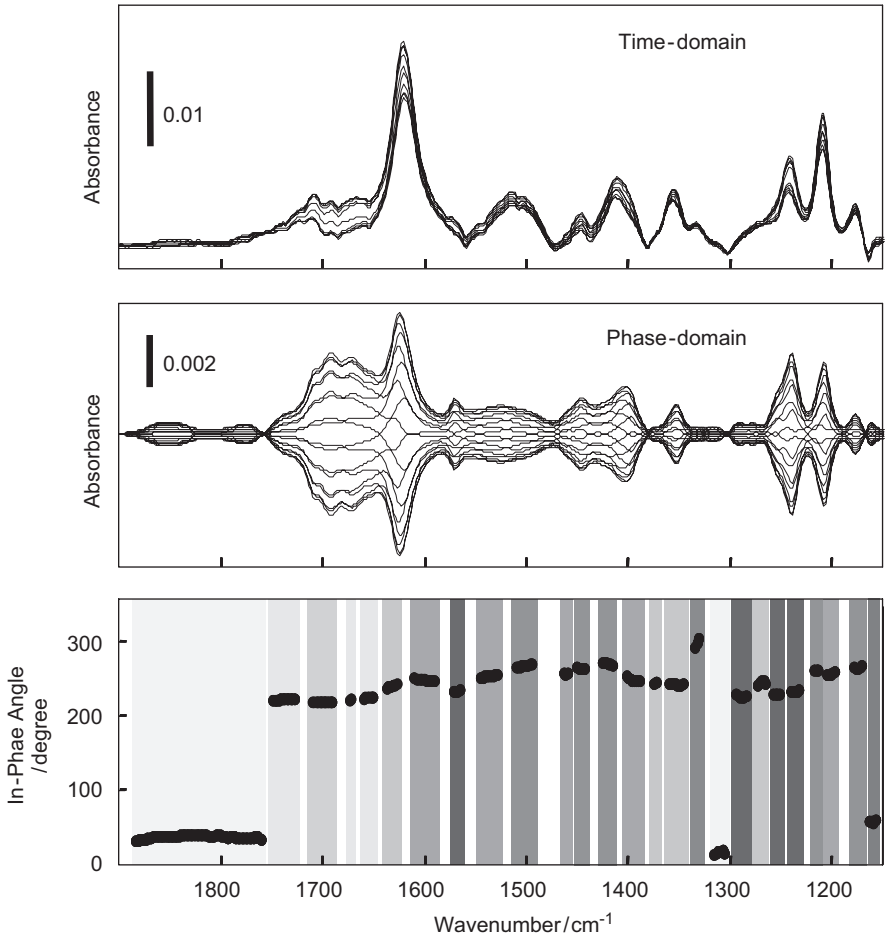

Fig. 6. Time- and phase-domain ATR spectra and in-phase demodulation angle plot of a modulation experiment. The concentration of the pyrone reactant **1** (see Fig. 7) was modulated between 0 and 3.6 mmol/l with a modulation period of 448 s. Solvent: hydrogen-saturated isopropanol; catalyst: 5 wt% Pd/TiO_2. For the time-domain spectra the reference was recorded before starting the modulation. The spectra are shown at T/10 and 20° time- and phase-domain interval, respectively. The different gray scale in the in-phase angle plot corresponds to the bands with the same phase delay, i.e. from the same species or different species appearing at the same time. The detailed band assignments are given in the original work (Bürgi and Baiker, 2002).

frequencies, allowing efficient frequency response analysis of active species by square-wave stimulation. Also, the high frequency demodulation using square-wave stimulation can be utilized in finding optimum experimental modulation frequency to separate active species of interests. In order to separate and identify signals appearing during a modulation cycle, it is desired to achieve kinetic differentiation as shown in Fig. 5. In the example of Fig. 5, we would not see a good separation of the bands in the spectra for A, B and C with $k\omega$ frequency demodulation when the MES experiment is done at a very low modulation frequency due to the too large time constants of the stimulation compared to the time constant of the reaction. Even in such a situation, we may obtain good separation of signals as in Fig. 5 by high frequency demodulation. In practice, if we carry out an experiment at ω frequency with square-wave stimulation and wish to estimate the amplitude and phase delay at higher $(2n-1)\omega$ frequencies, then we can take the phase delay as is, φ^{SW}_{2n-1} , and the amplitude multiplied by the factor of $2n-1$, $(2n-1)A^{SW}_{2n-1}$, after the $(2n-1)\omega$ frequency demodulation.

In summary, the fundamental frequency ($k=1$ in Eq. (1)) phase-domain analysis would yield equivalent information using sinusoidal- or square-wave stimulation. Moreover, high frequency demodulation can speed up the analysis of kinetics and facilitate the kinetic separation, hence the identification of species and their pathways during a modulation cycle.

4. Example: Enantioselective hydrogenation at a solid–liquid interface

The practical advantages shown above lead to a wide range of applications of MES, for example in biological systems (Fringeli, 1992; Müller et al., 1996; Fringeli et al., 2000; Baurecht et al., 2002), chiral recognition (Wirz et al., 2003, 2004; Bieri and Bürgi, 2005, 2006; Bieri et al., 2007), mass transfer (Urakawa et al., 2003; Urakawa et al., 2006b), photoreaction (Forster et al., 1976), and heterogeneous catalysis (Bürgi and Baiker, 2002; Gisler et al., 2003, 2004; Urakawa et al., 2006b). MES can be combined with any detection methods with a reasonable time-resolution. In heterogeneous

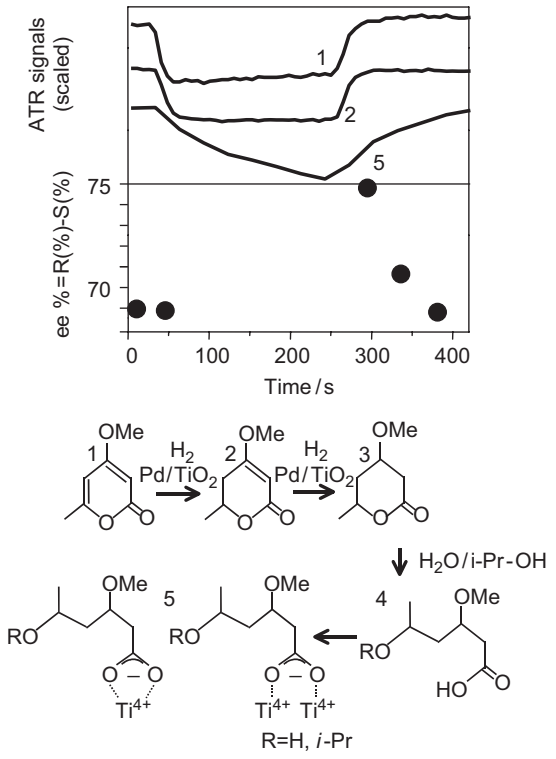

Fig. 7. Selected ATR signals as well as enantiomeric excess (ee, solid circles, determined by GC analysis, Bürgi and Baiker, 2002) as a function of time for the experiment shown in Fig. 6. ATR signals are shown of the reactant **1**, the primary hydrogenation product **2** and carboxylates adsorbed on TiO_2 **5**. Bottom: reactions observed by in situ ATR spectroscopy. Reprinted with permission from Bürgi and Baiker (2002). Copyright (2002) American Chemical Society.

catalysis, detection techniques very sensitive to surfaces, ATR-IR spectroscopy (Bürgi and Baiker, 2002; Gisler et al., 2003, 2004) and PM-IRRAS (Urakawa et al., 2006b), have been combined with MES to study solid–liquid and solid–gas interfaces, respectively. Here, we show as an example the investigation of a solid–liquid catalytic interface, the enantioselective hydrogenation of a pyrone over a cinchonidine-modified Pd/TiO_2 catalyst probed by ATR-IR spectroscopy (Bürgi and Baiker, 2002).

Fig. 6 shows time- and phase-domain ATR-IR spectra obtained by modulating the pyrone concentration keeping the modifier, cinchonidine, concentration constant. Most of the signals observed in the time-domain spectra are static, meaning that the species associated with these signals are not affected by the stimulation. It is indeed a very difficult task to investigate which bands are appearing when and understand the reaction pathway by the time-domain spectra. On the other hand, the phase-domain spectra remove all static signals in addition to noise, hence the signal to noise ratio has been significantly improved (another example of excellent sensitivity enhancement especially by noise removal can be found in, Gisler et al. (2003)). We can discriminate the species appearing at different time from the phase-domain spectra, e.g. when bands become maximum, i.e. in-phase. One way to conduct kinetic differentiation is shown in Fig. 6, using the plot of wavenumber versus in-phase angle, which clearly indicates the presence of several species during the course of the reaction. As mentioned before, the in-phase angle is correlated with the phase delay, hence such a plot would directly give information of the reaction pathway in addition to the kinetic differentiation. Fig. 7 shows the findings of the study. The first double bond is hydrogenated fast, whereas the second double bond leading to the lactone **3** is hydrogenated in a slower subsequent step. The lactone can furthermore hydrolyse, which results in the free carboxylic acid **4**. The latter accumulates as carboxylate on the catalyst surface. Analysis of the dissolved products at the outlet of the ATR cell revealed that the enantiomeric excess (ee) is not constant during the modulation period. The ee is initially high (75%) when the pyrone is admitted to the cell and decreases afterwards to a lower steady-state value (Fig. 7). The similar kinetics of this decay and the accumulation of the carboxylate on the catalyst surface, indicated that the latter hinders enantiodifferentiation. More details of the experimental conditions and results are in Bürgi and Baiker (2002).

5. Conclusions

Modulation excitation spectroscopy (MES) is a very powerful tool to sensitively monitor and identify active species occurring in a catalytic cycle. MES can be combined with any time-resolved detection technique which should be chosen according to the system and process of interest. It allows one to monitor only active species and remove signals due to spectators by the detection method, phase-sensitive detection (PSD), introducing additionally selectivity by a proper choice of an external perturbation parameter, the stimulation. Common stimulation shapes are sinusoidal- and square-waves. Data analysis obtained by MES experiments using the two types of stimulation can be handled in the same manner qualitatively and quantitatively, while in fact the response to square-wave stimulation contains richer but complex information. By PSD at multiple odd frequency, $(2n-1)\omega$, of the fundamental modulation frequency ω, we can take apart the rich information into different frequency components, thus accelerating dynamic behavior analysis of active species and also facilitating the kinetic separation of signals. The technique has already shown its usefulness in heterogeneous catalysis, and it is anticipated to become even a more important and practical tool in the future when more realistic, hence more complex, reactions are studied by *in situ* spectroscopy under working conditions.

References

Backus, E.H.G., Eichler, A., Kleyn, A.W., Bonn, M., 2005. Real-time observation of molecular motion on a surface. Science 310 (5755), 1790–1793.

Bauer, M., Lei, C., Read, K., Tobey, R., Gland, J., Murnane, M.M., Kapteyn, H.C., 2001. Direct observation of surface chemistry using ultrafast soft-X-ray pulses. Physical Review Letters 87 (2), 025501.

Baurecht, D., Fringeli, U.P., 2001. Quantitative modulated excitation Fourier transform infrared spectroscopy. Review of Scientific Instruments 72 (10), 3782–3792.

Baurecht, D., Porth, I., Fringeli, U.P., 2002. A new method of phase sensitive detection in modulation spectroscopy applied to temperature induced folding and unfolding of RNase A. Vibrational Spectroscopy 30 (1), 85–92.

Bieri, M., Bürgi, T., 2005. Probing enantiospecific interactions between proline and an L-glutathione self-assembled monolayer by modulation excitation ATR-IR spectroscopy. Journal of Physical Chemistry B 109 (20), 10243–10250.

Bieri, M., Bürgi, T., 2006. Enantiodiscrimination between an N-acetyl-L-cysteine SAM and proline: an in situ spectroscopic and computational study. ChemPhysChem 7 (2), 514–523.

Bieri, M., Gautier, C., Bürgi, T., 2007. Probing chiral interfaces by infrared spectroscopic methods. Physical Chemistry Chemical Physics 9 (6), 671–685.

Bürgi, T., Baiker, A., 2002. In situ infrared spectroscopy of catalytic solid–liquid interfaces using phase-sensitive detection: enantioselective hydrogenation of a pyrone over Pd/TiO_2. Journal of Physical Chemistry B 106 (41), 10649–10658.

Chenevarin, S., Thibault-Starzyk, F., 2004. Two-dimensional IR pressure-jump spectroscopy of adsorbed species for zeolites. Angewandte Chemie-International Edition 43 (9), 1155–1158.

Desamero, R., Rozovsky, S., Zhadin, N., McDermott, A., Callender, R., 2003. Active site loop motion in triosephosphate isomerase: T-jump relaxation spectroscopy of thermal activation. Biochemistry 42 (10), 2941–2951.

Forster, M., Loth, K., Andrist, M., Fringeli, U.P., Günthard, H.H., 1976. Kinetic study of photooxidation of pyrocatechol by modulated electronic excitation IR and ESR spectroscopy (MEIR and MESR). Chemical Physics 17 (1), 59–80.

Fringeli, U.P., 1992. In situ infrared attenuated total reflection membrane spectroscopy. Internal Reflection Spectroscopy Theory and Applications. J. F. M. Mirabella. New York, Dekker, pp. 255–324.

Fringeli, U.P., Baurecht, D., Günthard, H.H., 2000. Infrared and Raman Spectroscopy of Biological Materials. Infrared and Raman Spectroscopy of Biological Materials. H. U. Gremlich and B. Yan. New York/Basel, Dekker, pp. 143–192.

Gisler, A., Bürgi, T., Baiker, A., 2003. Epoxidation on titania-silica aerogel catalysts studied by attenuated total reflection Fourier transform infrared and modulation spectroscopy. Physical Chemistry Chemical Physics 5 (16), 3539–3548.

Gisler, A., Bürgi, T., Baiker, A., 2004. Epoxidation of cyclic allylic alcohols on titania-silica aerogels studied by attenuated total reflection infrared and modulation spectroscopy. Journal of Catalysis 222 (2), 461–469.

Gleaves, J.T., Ebner, J.R., Kuechler, T.C., 1988. Temporal analysis of products (TAP)—a unique catalyst evaluation system with submillisecond time resolution. Catalysis Reviews—Science and Engineering 30 (1), 49–116.

Hunger, M., Weitkamp, J., 2001. In situ IR, NMR, EPR, and UV/Vis spectroscopy: tools for new insight into the mechanisms of heterogeneous catalysis. Angewandte Chemie-International Edition 40 (16), 2954–2971.

Müller, M., Buchet, R., Fringeli, U.P., 1996. 2D-FTIR ATR spectroscopy of thermo-induced periodic secondary structural changes of poly-(L)-lysine: a cross-correlation analysis of phase-resolved temperature modulation spectra. Journal of Physical Chemistry 100 (25), 10810–10825.

Onyestyák, G., Valyon, J., Rees, L.V.C., 2000. A frequency-response study of the acidity of mordenite catalysts. Physical Chemistry Chemical Physics 2 (13), 3077–3082.

Pospíšil, P., Haumann, M., Dittmer, J., Solé, V.A., Dau, H., 2003. Stepwise transition of the tetra-manganese complex of photosystem II to a binuclear $Mn_2(\mu\text{–}O)_2$ complex in response to a temperature jump: a time-resolved structural investigation employing X-ray absorption spectroscopy. Biophysical Journal 84 (2), 1370–1386.

Urakawa, A., Wirz, R., Bürgi, T., Baiker, A., 2003. ATR-IR flow-through cell for concentration modulation excitation spectroscopy: diffusion experiments and simulations. Journal of Physical Chemistry B 107 (47), 13061–13068.

Urakawa, A., Bürgi, T., Baiker, A., 2006a. Kinetic analysis using square-wave stimulation in modulation excitation spectroscopy: mixing property of a flow-through PM-IRRAS Cell. Chemical Physics 324 (2–3), 653.

Urakawa, A., Bürgi, T., Schläpfer, H.-P., Baiker, A., 2006b. Simultaneous in situ monitoring of surface and gas species and surface properties by modulation excitation PM-IRRAS: CO oxidation over Pt film. Journal of Chemical Physics 124, 054717.

Weckhuysen, B.M., 2002. Snapshots of a working catalyst: possibilities and limitations of in situ spectroscopy in the field of heterogeneous catalysis. Chemical Communications 2, 97–110.

Wirz, R., Bürgi, T., Baiker, A., 2003. Probing enantiospecific interactions at chiral solid–liquid interfaces by absolute configuration modulation infrared spectroscopy. Langmuir 19 (3), 785–792.

Wirz, R., Bürgi, T., Lindner, W., Baiker, A., 2004. Absolute configuration modulation attenuated total reflection IR spectroscopy: an *in situ* method for probing chiral recognition in liquid chromatography. Analytical Chemistry 76 (18), 5319–5330.

Yablonsky, G.S., Olea, M., Marin, G.B., 2003. Temporal analysis of products: basic principles, applications, and theory. Journal of Catalysis 216 (1–2), 120–134.